ELSEVIER

International Journal of Solids and Structures 41 (2004) 1961–1974

INTERNATIONAL JOURNAL OF SOLIDS and STRUCTURES

www.elsevier.com/locate/ijsolstr

Thermal postbuckling behavior of functionally graded cylindrical shells with temperature-dependent properties

Hui-Shen Shen *

School of Civil Engineering and Mechanics, Shanghai Jiao Tong University, 1954 Hua Shan Road, Shanghai 200030, PR China

Received 12 March 2003; received in revised form 14 October 2003

Abstract

Thermal postbuckling analysis is presented for a functionally graded cylindrical thin shell of finite length. The temperature field considered is assumed to be a uniform distribution over the shell surface and through the shell thickness. Material properties are assumed to be temperature-dependent, and graded in the thickness direction according to a simple power law distribution in terms of the volume fractions of the constituents. The governing equations are based on the classical shell theory with a von Kármán–Donnell-type of kinematic nonlinearity. The nonlinear prebuckling deformations and initial geometric imperfections of the shell are both taken into account. A boundary layer theory of shell buckling, which includes the effects of nonlinear prebuckling deformations, large deflections in the postbuckling range, and initial geometric imperfections of the shell, is extended to the case of functionally graded cylindrical shells of finite length. A singular perturbation technique is employed to determine buckling temperature and postbuckling load–deflection curves. The numerical illustrations concern the thermal postbuckling response of perfect and imperfect, cylindrical thin shells with two constituent materials. The effects played by volume fraction distribution, and initial geometric imperfections are studied.

Keywords: Functionally graded materials; Temperature-dependent properties; Thermal postbuckling; Boundary layer theory of shell buckling; Singular perturbation technique

1. Introduction

Designs of airframes for high speed flight and spacecraft structures have to consider carefully the effect of the thermal environment on structural and material behavior. For this reason, many thermal postbuckling studies of composite laminated shell structures are available in the literature, see for example, Birman and Bert (1993), and Shen (1997, 2002a). In these studies the material properties are considered to be independent of temperature. Functionally graded materials (FGMs) are microscopically inhomogeneous composites usually made from a mixture of metals and ceramics. By gradually varying the volume fraction of the constituent materials, their material properties exhibit a smooth and continuous change from one

* Tel.: +86-2162-933081; fax: +86-2162-933021.
E-mail address: hsshen@mail.sjtu.edu.cn (H.-S. Shen).

0020-7683/$ - see front matter © 2003 Elsevier Ltd. All rights reserved.
doi:10.1016/j.ijsolstr.2003.10.023

surface to another, thus eliminating interface problems and mitigating thermal stress concentrations. FGMs are now developed for general use as structural components in extremely high temperature environments, and they have the advantage of being able to withstand high temperature environments while maintaining their structural integrity. Loy et al. (1999) presented a free vibration analysis of simply supported FGM cylindrical thin shells. This work was then extended to the case of FGM cylindrical thin shells under various boundary conditions by Pradhan et al. (2000). Gong et al. (1999) gave an elastic response analysis of simply supported FGM cylindrical shells under low-velocity impact. By using the finite element method and Fourier transformation technique, Han et al. (2001) solved the wave motion in an FGM cylinder. Ng et al. (2001) studied the parametric resonance or dynamic stability of FGM cylindrical thin shells under periodic axial loading. In the forgoing studies, Reddy and his co-workers developed a simple theory, in which the material properties are graded in the thickness direction according to a volume fraction power law distribution, but their numerical results were only for a simple case of an FGM shell in a constant thermal environment. Recently, Shen (2002b, 2003) gave a postbuckling analysis of FGM cylindrical thin shells subjected to axial compression or external pressure. In the above studies, the material properties were considered to be temperature-dependent and the effect of temperature rise on the postbuckling behavior was reported. Also recently, Shahsiah and Eslami (2003) studied the thermal buckling of FGM cylindrical shells under two types of thermal loads based on the first order shear deformation shell theory. In their analysis the material properties were considered to be independent of temperature. However, studies on thermal postbuckling of FGM cylindrical shells with temperature-dependent thermoelastic properties have not been seen in the literature. This problem is studied in the present paper, for the case when two end edges of the shell are assumed to be simply supported or clamped with no in-plane displacement.

Under the present study, the material properties are assumed to be nonlinear functions of temperature, and graded in the thickness direction according to a volume fraction power law distribution. It is because the thermal buckling only occurs for thin cylindrical shells. The governing equations are based on the classical shell theory with a von Kármán–Donnell-type of kinematic nonlinearity. The boundary layer theory suggested by Shen and Chen (1988, 1990) is extended to the case of FGM cylindrical shells with two constituent materials subjected to a uniform temperature rise. A singular perturbation technique is employed to determine the buckling temperature and thermal postbuckling load–deflection curves. The nonlinear prebuckling deformations and initial geometric imperfections of the shell are both taken into account but, for simplicity, the form of initial geometric imperfection is assumed to be the same as the initial buckling mode of the shell.

2. Theoretical development

Consider an FGM circular cylindrical shell with mean radius R, length L and thickness t, which is made from a mixture of ceramic and metallic materials. The shell is referred to a coordinate system (X, Y, Z) in which X and Y are in the axial and circumferential directions of the shell and Z is in the direction of the inward normal to the middle surface. The corresponding displacements are designated by $\overline{U}$, $\overline{V}$ and $\overline{W}$. The origin of the coordinate system is located at the end of the shell in the middle plane. The shell is assumed to be relatively thin and geometrically imperfect, and is subjected to a uniform temperature rise ΔT. Denoting the initial geometric imperfection by $\overline{W}^*(X, Y)$, let $\overline{W}(X, Y)$ be the additional deflection and $\overline{F}(X, Y)$ be the stress function for the stress resultants defined by $\overline{N}_x = \overline{F}_{,yy}$, $\overline{N}_y = \overline{F}_{,xx}$ and $\overline{N}_{xy} = -\overline{F}_{,xy}$, where a comma denotes partial differentiation with respect to the corresponding coordinates.

Assume that the material composition varies smoothly from the outer to the inner surface of the shell. In such a way, the effective material properties P, like Young's modulus E or thermal expansion coefficient α, can be expressed as

$$P = P_o V_o + P_i V_i \tag{1}$$

where P_o and P_i denote the temperature-dependent properties of the outer and inner surfaces of the shell, respectively, and V_o and V_i are the volume fractions of the constituent materials corresponding to P_o and P_i and are related by

$$V_o + V_i = 1 \tag{2}$$

The volume fraction V_i follows a simple power law

$$V_i = \left(\frac{2Z+t}{2t}\right)^N \tag{3}$$

where volume fraction index N dictates the material variation profile through the shell thickness and may be varied to obtain the optimum distribution of component materials. It is evident that when $N = 0$, $V_i = 1$ and $V_o = 0$, the shell is an isotropic one made up of material as that at the inner surface.

From Eqs. (1)–(3), the effective Young's modulus E and thermal expansion coefficient α of an FGM cylindrical shell can be written as (see Gibson et al., 1995)

$$\begin{aligned} E(Z,T) &= [E_i(T) - E_o(T)]\left(\frac{2Z+t}{2t}\right)^N + E_o(T) \\ \alpha(Z,T) &= [\alpha_i(T) - \alpha_o(T)]\left(\frac{2Z+t}{2t}\right)^N + \alpha_o(T) \end{aligned} \tag{4}$$

It is evident that when $Z = -t/2$, $E = E_o$ and $\alpha = \alpha_o$, and when $Z = t/2$, $E = E_i$ and $\alpha = \alpha_i$. Since functionally graded structures are most commonly used in high temperature environment where significant changes in mechanical properties of the constituent materials are to be expected (see Reddy and Chin, 1998), it is essential to take into consideration this temperature-dependency for accurate prediction of the mechanical response. Thus, E_o, E_i, α_o and α_i are functions of temperature, as to be shown in Section 4, so that E and α are both temperature and position dependent.

Based on classical shell theory (i.e. transverse shear deformation effects are neglected) with von Kármán–Donnell-type kinematic relations and including thermal effects, the governing differential equations for an FGM cylindrical shell have been derived and can be expressed in terms of a stress function $\overline{F}$, the transverse displacement $\overline{W}$, and the initial geometric imperfection $\overline{W}^*$. They are

$$\tilde{L}_{11}(\overline{W}) + \tilde{L}_{12}(\overline{F}) - \tilde{L}_{13}(\overline{N}^T) - \tilde{L}_{14}(\overline{M}^T) - \frac{1}{R}\overline{F}_{,xx} = \tilde{L}(\overline{W} + \overline{W}^*, \overline{F}) \tag{5}$$

$$\tilde{L}_{21}(\overline{F}) - \tilde{L}_{22}(\overline{W}) - \tilde{L}_{23}(\overline{N}^T) + \frac{1}{R}\overline{W}_{,xx} = -\frac{1}{2}\tilde{L}(\overline{W} + 2\overline{W}^*, \overline{W}) \tag{6}$$

where the linear operators $\tilde{L}_{ij}(\ )$ and the nonlinear operator $\tilde{L}(\ )$ are defined as

$$
\begin{aligned}
\tilde{L}_{11}(\ ) &= D_{11}^{*}\frac{\partial^4}{\partial X^4} + 2(D_{12}^{*} + 2D_{66}^{*})\frac{\partial^4}{\partial X^2 \partial Y^2} + D_{22}^{*}\frac{\partial^4}{\partial Y^4} \\
\tilde{L}_{12}(\ ) &= \tilde{L}_{22}(\ ) = B_{21}^{*}\frac{\partial^4}{\partial X^4} + (B_{11}^{*} + B_{22}^{*} - 2B_{66}^{*})\frac{\partial^4}{\partial X^2 \partial Y^2} + B_{12}^{*}\frac{\partial^4}{\partial Y^4} \\
\tilde{L}_{13}(\overline{N}^{T}) &= \frac{\partial^2}{\partial X^2}(B_{11}^{*}\overline{N}_{x}^{T} + B_{21}^{*}\overline{N}_{y}^{T}) + 2\frac{\partial^2}{\partial X \partial Y}(B_{66}^{*}\overline{N}_{xy}^{T}) + \frac{\partial^2}{\partial Y^2}(B_{12}^{*}\overline{N}_{x}^{T} + B_{22}^{*}\overline{N}_{y}^{T}) \\
\tilde{L}_{14}(\overline{M}^{T}) &= \frac{\partial^2}{\partial X^2}(\overline{M}_{x}^{T}) + 2\frac{\partial^2}{\partial X \partial Y}(\overline{M}_{xy}^{T}) + \frac{\partial^2}{\partial Y^2}(\overline{M}_{y}^{T}) \\
\tilde{L}_{21}(\ ) &= A_{22}^{*}\frac{\partial^4}{\partial X^4} + (2A_{12}^{*} + A_{66}^{*})\frac{\partial^4}{\partial X^2 \partial Y^2} + A_{11}^{*}\frac{\partial^4}{\partial Y^4} \\
\tilde{L}_{23}(\overline{N}^{T}) &= \frac{\partial^2}{\partial X^2}(A_{12}^{*}\overline{N}_{x}^{T} + A_{22}^{*}\overline{N}_{y}^{T}) - \frac{\partial^2}{\partial X \partial Y}(A_{66}^{*}\overline{N}_{xy}^{T}) + \frac{\partial^2}{\partial Y^2}(A_{11}^{*}\overline{N}_{x}^{T} + A_{12}^{*}\overline{N}_{y}^{T}) \\
\tilde{L}(\ ) &= \frac{\partial^2}{\partial X^2}\frac{\partial^2}{\partial Y^2} - 2\frac{\partial^2}{\partial X \partial Y}\frac{\partial^2}{\partial X \partial Y} + \frac{\partial^2}{\partial Y^2}\frac{\partial^2}{\partial X^2}
\end{aligned}
\tag{7}
$$

It is noted that these shell equations include thermal coupling as well as the interaction of stretching and bending. Eqs. (5)–(7) are identical in form to those of unsymmetric cross-ply laminated cylindrical shells under thermomechanical loading (see Shen, 1997), but now all the reduced stiffness matrices $[A_{ij}^{*}]$, $[B_{ij}^{*}]$ and $[D_{ij}^{*}]$ $(i, j = 1, 2, 6)$ are functions of temperature and position, defined by

$$
\mathbf{A}^{*} = \mathbf{A}^{-1}, \quad \mathbf{B}^{*} = -\mathbf{A}^{-1}\mathbf{B}, \quad \mathbf{D}^{*} = \mathbf{D} - \mathbf{B}\mathbf{A}^{-1}\mathbf{B} \tag{8}
$$

where A_{ij}, B_{ij} and D_{ij} are defined by

$$
(A_{ij}, B_{ij}, D_{ij}) = \int_{-t/2}^{t/2} (Q_{ij})(1, Z, Z^2)\,\mathrm{d}Z \quad (i, j = 1, 2, 6) \tag{9}
$$

and

$$
Q_{11} = Q_{22} = \frac{E(Z,T)}{1-\nu^2}, \quad Q_{12} = \frac{\nu E(Z,T)}{1-\nu^2}, \quad Q_{16} = Q_{26} = 0, \quad Q_{66} = \frac{E(Z,T)}{2(1+\nu)} \tag{10}
$$

in which E is given in detail in Eq. (4), and varies through the shell thickness.

The forces and moments caused by elevated temperature are defined by

$$
\begin{bmatrix} \overline{N}_{x}^{T} & \overline{M}_{x}^{T} \\ \overline{N}_{y}^{T} & \overline{M}_{y}^{T} \\ \overline{N}_{xy}^{T} & \overline{M}_{xy}^{T} \end{bmatrix} = \int_{-t/2}^{t/2} \begin{bmatrix} A_x(Z,T) \\ A_y(Z,T) \\ A_{xy}(Z,T) \end{bmatrix} \Delta T(1, Z)\,\mathrm{d}Z \tag{11}
$$

where ΔT is temperature rise from some reference temperature at which there are no thermal strains, and

$$
\begin{bmatrix} A_x(Z,T) \\ A_y(Z,T) \\ A_{xy}(Z,T) \end{bmatrix} = -\begin{bmatrix} Q_{11} & Q_{12} & Q_{16} \\ Q_{12} & Q_{22} & Q_{26} \\ Q_{16} & Q_{26} & Q_{66} \end{bmatrix} \begin{bmatrix} 1 & 0 \\ 0 & 1 \\ 0 & 0 \end{bmatrix} \begin{bmatrix} \alpha(Z,T) \\ \alpha(Z,T) \end{bmatrix} \tag{12}
$$

where the thermal expansion coefficient α is also given in detail in Eq. (4).

The two end edges of the shell are assumed to be simply supported or clamped, and to be restrained against expansion longitudinally while temperature is increased steadily, so that the boundary conditions are

$X = 0, L$:

$$
\overline{W} = 0 \tag{13a}
$$

$$
\overline{U} = 0 \tag{13b}
$$

$$\overline{M}_x = -B_{21}^* \frac{\partial^2 \overline{F}}{\partial X^2} - B_{11}^* \frac{\partial^2 \overline{F}}{\partial Y^2} - D_{11}^* \frac{\partial^2 \overline{W}}{\partial X^2} - D_{12}^* \frac{\partial^2 \overline{W}}{\partial Y^2} + \overline{M}_x^T = 0 \quad \text{(simply supported)} \tag{13c}$$

$$\overline{W} = \overline{W}_{,x} = 0 \quad \text{(clamped)} \tag{13d}$$

where $\overline{M}_x$ is the bending moment. Also, we have the closed (or periodicity) condition

$$\int_0^{2\pi R} \frac{\partial \overline{V}}{\partial Y} \, \mathrm{d}Y = 0 \tag{14a}$$

or

$$\int_0^{2\pi R} \left[A_{22}^* \frac{\partial^2 \overline{F}}{\partial X^2} + A_{12}^* \frac{\partial^2 \overline{F}}{\partial Y^2} - \left(B_{21}^* \frac{\partial^2 \overline{W}}{\partial X^2} + B_{22}^* \frac{\partial^2 \overline{W}}{\partial Y^2} \right) + \frac{\overline{W}}{R} - \frac{1}{2} \left(\frac{\partial \overline{W}}{\partial Y} \right)^2 - \frac{\partial \overline{W}}{\partial Y} \frac{\partial \overline{W}^*}{\partial Y} - (A_{12}^* \overline{N}_x^T + A_{22}^* \overline{N}_y^T) \right] \mathrm{d}Y = 0 \tag{14b}$$

Because of Eq. (14), the in-plane boundary condition $\overline{V} = 0$ (at $X = 0, L$) is not needed in Eq. (13).

The average end-shortening relationship is defined as

$$\begin{aligned} \frac{\Delta_x}{L} &= -\frac{1}{2\pi RL} \int_0^{2\pi R} \int_0^L \frac{\partial \overline{U}}{\partial X} \, \mathrm{d}X \, \mathrm{d}Y \\ &= -\frac{1}{2\pi RL} \int_0^{2\pi R} \int_0^L \left[A_{11}^* \frac{\partial^2 \overline{F}}{\partial Y^2} + A_{12}^* \frac{\partial^2 \overline{F}}{\partial X^2} - \left(B_{11}^* \frac{\partial^2 \overline{W}}{\partial X^2} + B_{12}^* \frac{\partial^2 \overline{W}}{\partial Y^2} \right) \right. \\ &\quad \left. - \frac{1}{2} \left(\frac{\partial \overline{W}}{\partial X} \right)^2 - \frac{\partial \overline{W}}{\partial X} \frac{\partial \overline{W}^*}{\partial X} - (A_{11}^* \overline{N}_x^T + A_{12}^* \overline{N}_y^T) \right] \mathrm{d}X \, \mathrm{d}Y \end{aligned} \tag{15}$$

3. Analytical method and asymptotic solutions

Having developed the theory, we are now in a position to solve Eqs. (5) and (6) with boundary condition (13). Before proceeding, it is convenient first to define the following dimensionless quantities

$$\begin{aligned} &x = \pi X/L, \quad y = Y/R, \quad \beta = L/\pi R, \quad \overline{Z} = L^2/Rt, \quad \varepsilon = (\pi^2 R/L^2)[D_{11}^* D_{22}^* A_{11}^* A_{22}^*]^{1/4} \\ &(W, W^*) = \varepsilon(\overline{W}, \overline{W}^*)/[D_{11}^* D_{22}^* A_{11}^* A_{22}^*]^{1/4}, \quad F = \varepsilon^2 \overline{F}/[D_{11}^* D_{22}^*]^{1/2} \\ &\gamma_{12} = (D_{12}^* + 2D_{66}^*)/D_{11}^*, \quad \gamma_{22} = (A_{12}^* + A_{66}^*/2)/A_{22}^* \\ &\gamma_{14} = [D_{22}^*/D_{11}^*]^{1/2}, \quad \gamma_{24} = [A_{11}^*/A_{22}^*]^{1/2}, \quad \gamma_5 = -A_{12}^*/A_{22}^* \\ &(\gamma_{30}, \gamma_{32}, \gamma_{34}, \gamma_{311}, \gamma_{322}) = (B_{21}^*, B_{11}^* + B_{22}^* - 2B_{66}^*, B_{12}^*, B_{11}^*, B_{22}^*)/[D_{11}^* D_{22}^* A_{11}^* A_{22}^*]^{1/4} \\ &(\gamma_{T1}, \gamma_{T2}) = (A_x^T, A_y^T) R [A_{11}^* A_{22}^*/D_{11}^* D_{22}^*]^{1/4} \\ &(M_x, M_x^T) = \varepsilon^2 \left(\overline{M}_x, \overline{M}_x^T \right) (L^2/\pi^2)/D_{11}^* [D_{11}^* D_{22}^* A_{11}^* A_{22}^*]^{1/4} \\ &\delta_x = \left(\frac{\Delta_x}{L} \right) \frac{R}{2[D_{11}^* D_{22}^* A_{11}^* A_{22}^*]^{1/4}}, \quad \lambda_T = \alpha_0 \Delta T \end{aligned} \tag{16}$$

where α_0 is an arbitrary reference value, and

$$\alpha_{11} = a_{11}\alpha_0, \quad \alpha_{22} = a_{22}\alpha_0 \tag{17}$$

in Eq. (16) $A_x^T = A_y^T$ are defined by

$$\begin{bmatrix} A_x^T \\ A_y^T \end{bmatrix} = -\int_{-t/2}^{t/2} \begin{bmatrix} A_x \\ A_y \end{bmatrix} \mathrm{d}Z \tag{18}$$

and the details of which can be found in Appendix A.

The nonlinear Eqs. (5) and (6) may then be written in dimensionless form as

$$\varepsilon^2 L_{11}(W) + \varepsilon\gamma_{14}L_{12}(F) - \gamma_{14}F_{,xx} = \gamma_{14}\beta^2 L(W + W^*, F) \tag{19}$$

$$L_{21}(F) - \varepsilon\gamma_{24}L_{22}(W) + \gamma_{24}W_{,xx} = -\tfrac{1}{2}\gamma_{24}\beta^2 L(W + 2W^*, W) \tag{20}$$

where

$$\begin{aligned}
L_{11}(\ ) &= \frac{\partial^4}{\partial x^4} + 2\gamma_{12}\beta^2\frac{\partial^4}{\partial x^2\partial y^2} + \gamma_{14}^2\beta^4\frac{\partial^4}{\partial y^4} \\
L_{12}(\ ) = L_{22}(\ ) &= \gamma_{30}\frac{\partial^4}{\partial x^4} + \gamma_{32}\beta^2\frac{\partial^4}{\partial x^2\partial y^2} + \gamma_{34}\beta^4\frac{\partial^4}{\partial y^4} \\
L_{21}(\ ) &= \frac{\partial^4}{\partial x^4} + 2\gamma_{22}\beta^2\frac{\partial^4}{\partial x^2\partial y^2} + \gamma_{24}^2\beta^4\frac{\partial^4}{\partial y^4} \\
L(\ ) &= \frac{\partial^2}{\partial x^2}\frac{\partial^2}{\partial y^2} - 2\frac{\partial^2}{\partial x\partial y}\frac{\partial^2}{\partial x\partial y} + \frac{\partial^2}{\partial y^2}\frac{\partial^2}{\partial x^2}
\end{aligned} \tag{21}$$

For most of the FGMs $[D_{11}^* D_{22}^* A_{11}^* A_{22}^*]^{1/4} \cong 0.3t$. Moreover, when $\overline{Z} = (L^2/Rt) > 2.96$, then from Eq. (16) $\varepsilon < 1$. In particular, for homogeneous isotropic cylindrical shells, $\varepsilon = \pi^2/\overline{Z}_B\sqrt{12}$, where $\overline{Z}_B = (L^2/Rt) \times [1 - \nu^2]^{1/2}$ is the Batdorf shell parameter, which should be greater than 2.85 in the case of classical linear buckling analysis (Batdorf, 1947). In practice, the shell structure will have $\overline{Z} \geqslant 10$, so that we always have $\varepsilon \ll 1$. When $\varepsilon < 1$, Eqs. (19) and (20) are of the boundary layer type, then nonlinear prebuckling deformations, large deflections in the postbuckling range, and initial geometric imperfections of the shell can be considered simultaneously.

The boundary conditions of Eq. (13) become

$x = 0, \pi$;

$$W = 0 \tag{22a}$$

$$\delta_x = 0 \tag{22b}$$

$$M_x = 0 \quad \text{(simply supported)} \tag{22c}$$

$$W_{,x} = 0 \quad \text{(clamped)} \tag{22d}$$

and the closed condition of Eq. (14b) becomes

$$\begin{aligned}
\int_0^{2\pi} \Bigg[&\left(\frac{\partial^2 F}{\partial x^2} - \gamma_5\beta^2\frac{\partial^2 F}{\partial y^2}\right) - \varepsilon\gamma_{24}\left(\gamma_{30}\frac{\partial^2 W}{\partial x^2} + \gamma_{322}\beta^2\frac{\partial^2 W}{\partial y^2}\right) + \gamma_{24}W - \frac{1}{2}\gamma_{24}\beta^2\left(\frac{\partial W}{\partial y}\right)^2 \\
&- \gamma_{24}\beta^2\frac{\partial W}{\partial y}\frac{\partial W^*}{\partial y} + \varepsilon(\gamma_{T2} - \gamma_5\gamma_{T1})\lambda_T \Bigg] \mathrm{d}y = 0
\end{aligned} \tag{23}$$

The unit end-shortening relationship becomes

$$\delta_x = -\frac{1}{4\pi^2\gamma_{24}}\varepsilon^{-1}\int_0^{2\pi}\int_0^{\pi}\left[\left(\gamma_{24}^2\beta^2\frac{\partial^2 F}{\partial y^2}-\gamma_5\frac{\partial^2 F}{\partial x^2}\right)-\varepsilon\gamma_{24}\left(\gamma_{311}\frac{\partial^2 W}{\partial x^2}+\gamma_{34}\beta^2\frac{\partial^2 W}{\partial y^2}\right)-\frac{1}{2}\gamma_{24}\left(\frac{\partial W}{\partial x}\right)^2 - \gamma_{24}\frac{\partial W}{\partial x}\frac{\partial W^*}{\partial x}+\varepsilon(\gamma_{24}^2\gamma_{T1}-\gamma_5\gamma_{T2})\lambda_T\right]\mathrm{d}x\,\mathrm{d}y \tag{24}$$

By virtue of the fact that ΔT is assumed to be uniform, the thermal coupling in Eqs. (5) and (6) vanishes, but the terms in ΔT affect Eqs. (23) and (24).

From Eqs. (19)–(24), one can determine the thermal postbuckling behavior of perfect and imperfect FGM cylindrical shells subjected to a uniform temperature rise by means of a singular perturbation technique. The essence of this procedure, in the present case, is to assume that

$$\begin{aligned} W &= w(x,y,\varepsilon)+\tilde{W}(x,\xi,y,\varepsilon)+\hat{W}(x,\zeta,y,\varepsilon)\\ F &= f(x,y,\varepsilon)+\tilde{F}(x,\xi,y,\varepsilon)+\hat{F}(x,\zeta,y,\varepsilon)\end{aligned} \tag{25}$$

where ε is a small perturbation parameter (provided $\overline{Z} > 2.96$) as defined in Eq. (16) and $w(x,y,\varepsilon)$, $f(x,y,\varepsilon)$ are called outer or regular solutions of the shell, $\tilde{W}(x,\xi,y,\varepsilon)$, $\tilde{F}(x,\xi,y,\varepsilon)$ and $\hat{W}(x,\zeta,y,\varepsilon)$, $\hat{F}(x,\zeta,y,\varepsilon)$ are the boundary layer solutions near the $x=0$ and $x=\pi$ edges, respectively, and ξ and ζ are the boundary layer variables, defined as

$$\xi = x/\sqrt{\varepsilon},\quad \zeta = (\pi-x)/\sqrt{\varepsilon} \tag{26}$$

This means for homogeneous isotropic cylindrical shells the width of the boundary layers is of order $\sqrt{Rt}$. In Eq. (25) the regular and boundary layer solutions are taken in the forms of perturbation expansions as

$$w(x,y,\varepsilon)=\sum_{j=1}\varepsilon^j w_j(x,y),\quad f(x,y,\varepsilon)=\sum_{j=0}\varepsilon^j f_j(x,y) \tag{27a}$$

$$\tilde{W}(x,\xi,y,\varepsilon)=\sum_{j=0}\varepsilon^{j+1}\tilde{W}_{j+1}(x,\xi,y),\quad \tilde{F}(x,\xi,y,\varepsilon)=\sum_{j=0}\varepsilon^{j+2}\tilde{F}_{j+2}(x,\xi,y) \tag{27b}$$

$$\hat{W}(x,\zeta,y,\varepsilon)=\sum_{j=0}\varepsilon^{j+1}\hat{W}_{j+1}(x,\zeta,y),\quad \hat{F}(x,\zeta,y,\varepsilon)=\sum_{j=0}\varepsilon^{j+2}\hat{F}_{j+2}(x,\zeta,y) \tag{27c}$$

The initial buckling mode is assumed to have the form

$$w_2(x,y)=A_{11}^{(2)}\sin mx\sin ny \tag{28}$$

and the initial geometric imperfection is assumed to have the similar form

$$W^*(x,y,\varepsilon)=\varepsilon^2 a_{11}^*\sin mx\sin ny=\varepsilon^2\propto A_{11}^{(2)}\sin mx\sin ny \tag{29}$$

where $\propto = a_{11}^*/A_{11}^{(2)}$ is the imperfection parameter.

Substituting Eqs. (25)–(27) into Eqs. (19) and (20) and collecting terms of the same order of ε, one obtains three sets of perturbation equations for the regular and boundary layer solutions respectively.

Using Eqs. (28) and (29) to solve these perturbation equations of each order, and matching the regular solutions with the boundary layer solutions at each end of the shell, one has the asymptotic solutions satisfying the clamped boundary conditions. They are

$$W = \varepsilon\left[A_{00}^{(1)} - A_{00}^{(1)}\left(\cos\phi\frac{x}{\sqrt{\varepsilon}} + \frac{\vartheta}{\phi}\sin\phi\frac{x}{\sqrt{\varepsilon}}\right)\exp\left(-\vartheta\frac{x}{\sqrt{\varepsilon}}\right) - A_{00}^{(1)}\left(\cos\phi\frac{\pi-x}{\sqrt{\varepsilon}} + \frac{\vartheta}{\phi}\sin\phi\frac{\pi-x}{\sqrt{\varepsilon}}\right)\exp\left(-\vartheta\frac{\pi-x}{\sqrt{\varepsilon}}\right)\right] + \varepsilon^2\left[A_{11}^{(2)}\sin mx\sin ny + A_{02}^{(2)}\cos 2ny - (A_{02}^{(2)}\cos 2ny)\left(\cos\phi\frac{x}{\sqrt{\varepsilon}} + \frac{\vartheta}{\phi}\sin\phi\frac{x}{\sqrt{\varepsilon}}\right)\exp\left(-\vartheta\frac{x}{\sqrt{\varepsilon}}\right) - (A_{02}^{(2)}\cos 2ny)\left(\cos\phi\frac{\pi-x}{\sqrt{\varepsilon}} + \frac{\vartheta}{\phi}\sin\phi\frac{\pi-x}{\sqrt{\varepsilon}}\right)\exp\left(-\vartheta\frac{\pi-x}{\sqrt{\varepsilon}}\right)\right] + \varepsilon^3[A_{11}^{(3)}\sin mx\sin ny + A_{02}^{(3)}\cos 2ny] + \varepsilon^4[A_{00}^{(4)} + A_{11}^{(4)}\sin mx\sin ny + A_{20}^{(4)}\sin 2mx + A_{02}^{(4)}\cos 2ny + A_{13}^{(4)}\sin mx\sin 3ny + A_{04}^{(4)}\cos 4ny] + \mathrm{O}(\varepsilon^5) \tag{30}$$

$$F = -B_{00}^{(0)}\frac{y^2}{2} + \varepsilon\left[-B_{00}^{(1)}\frac{y^2}{2}\right] + \varepsilon^2\left[-B_{00}^{(2)}\frac{y^2}{2} + B_{11}^{(2)}\sin mx\sin ny + A_{00}^{(1)}\left(b_{01}^{(2)}\cos\phi\frac{x}{\sqrt{\varepsilon}} + b_{10}^{(2)}\sin\phi\frac{x}{\sqrt{\varepsilon}}\right)\exp\left(-\vartheta\frac{x}{\sqrt{\varepsilon}}\right) + A_{00}^{(1)}\left(b_{01}^{(2)}\cos\phi\frac{\pi-x}{\sqrt{\varepsilon}} + b_{10}^{(2)}\sin\phi\frac{\pi-x}{\sqrt{\varepsilon}}\right) \times \exp\left(-\vartheta\frac{\pi-x}{\sqrt{\varepsilon}}\right)\right] + \varepsilon^3\left[-B_{00}^{(3)}\frac{y^2}{2} + B_{02}^{(3)}\cos 2ny + (A_{02}^{(2)}\cos 2ny)\left(b_{01}^{(3)}\cos\phi\frac{x}{\sqrt{\varepsilon}} + b_{10}^{(3)}\sin\phi\frac{x}{\sqrt{\varepsilon}}\right) \times \exp\left(-\vartheta\frac{x}{\sqrt{\varepsilon}}\right) + (A_{02}^{(2)}\cos 2ny)\left(b_{01}^{(3)}\cos\phi\frac{\pi-x}{\sqrt{\varepsilon}} + b_{10}^{(3)}\sin\phi\frac{\pi-x}{\sqrt{\varepsilon}}\right) \times \exp\left(-\vartheta\frac{\pi-x}{\sqrt{\varepsilon}}\right)\right] + \varepsilon^4\left[-B_{00}^{(4)}\frac{y^2}{2} + B_{20}^{(4)}\cos 2mx + B_{02}^{(4)}\cos 2ny + B_{13}^{(4)}\sin mx\sin 3ny\right] + \mathrm{O}(\varepsilon^5) \tag{31}$$

Note that, because of Eq. (30), the prebuckling deformation of the shell is nonlinear, and all of the coefficients in Eqs. (30) and (31) are related and can be expressed in terms of $A_{11}^{(2)}$, but for the sake of brevity the detailed expressions are not shown, whereas ϑ and ϕ are given in detail in Appendix A.

Next, upon substitution of Eqs. (30) and (31) into the boundary condition (22b) and into closed condition (23) and Eq. (24), the thermal postbuckling equilibrium path can be written as

$$\lambda_T = C_{11}[\lambda_T^{(0)} - \lambda_T^{(2)}(A_{11}^{(2)}\varepsilon)^2 + \lambda_T^{(4)}(A_{11}^{(2)}\varepsilon)^4 + \cdots] \tag{32}$$

In Eq. (32), $(A_{11}^{(2)}\varepsilon)$ is taken as the second perturbation parameter relating to the dimensionless maximum deflection. If the maximum deflection is assumed to be at the point $(x, y) = (\pi/2m, \pi/2n)$, from Eq. (30) one has

$$A_{11}^{(2)}\varepsilon = W_m - \Theta_3 W_m^2 + \cdots \tag{33a}$$

where W_m is the dimensionless form of the maximum deflection of the shell that can be written as

$$W_m = \frac{1}{C_3}\left[\frac{t}{[D_{11}^* D_{22}^* A_{11}^* A_{22}^*]^{1/4}}\frac{\overline{W}}{t} + \Theta_4\right] \tag{33b}$$

All symbols used in Eqs. (32) and (33) are also described in detail in Appendix A. It is noted that $\lambda_T^{(i)}$ $(i = 0, 2, \ldots)$ are all functions of temperature and position.

4. Numerical results and discussion

Numerical results are presented in this section for FGM cylindrical shells with two constituent materials. Two sets of material mixture are considered. One is silicon nitride and stainless steel and the other is zirconium oxide and titanium alloy. Two types of FGM cylindrical shell, Type A and Type B, are configurated. For Type A, the outer surface of the shell is ceramic-rich and the inner surface is metal-rich (referred to as Si_3N_4/SUS304 or ZrO_2/Ti–6Al–4V). For Type B, the outer surface of the shell is metal-rich and the inner surface is ceramic-rich (referred to as SUS304/Si_3N_4 or Ti–6Al–4V/ZrO_2). The material properties P, such as Young's modulus E and thermal expansion coefficient α, can be expressed as a nonlinear function of temperature (see Touloukian, 1967) as

$$P = P_0(P_{-1}T^{-1} + 1 + P_1T + P_2T^2 + P_3T^3) \tag{34}$$

in which $T = T_0 + \Delta T$ and $T_0 = 300$ K (room temperature), P_0, P_{-1}, P_1, P_2 and P_3 are the coefficients of temperature T (K) and are unique to the constituent materials. Typical values for the Young's modulus E (in Pa) and the thermal expansion coefficient α (in K) of these materials are listed in Table 1 (from Reddy and Chin, 1998). Poisson's ratio v is assumed to be a constant, and $v = 0.28$.

To obtain numerical results, it is necessary to solve Eq. (32) by an iterative numerical procedure with the following steps:

(1) Begin with $\overline{W}/t = 0$.
(2) Assume elastic constants and the thermal expansion coefficients are constant, i.e. at $T_0 = 300$ K. The thermal buckling load for the shell of temperature-independent material is obtained.

Table 1
Temperature-dependent coefficients E (in Pa) and α (in K) for ceramics and metals (from Reddy and Chin, 1998)

Materials		P_0	P_{-1}	P_1	P_2	P_3
Zirconia	E	244.27e+9	0	−1.371e−3	1.214e−6	−3.681e−10
	α	12.766e−6	0	−1.491e−3	1.006e−5	−6.778e−11
Silicon nitride	E	348.43e+9	0	−3.070e−4	2.160e−7	−8.946e−11
	α	5.8723e−6	0	9.095e−4	0	0
Ti–6Al–4V	E	122.56e+9	0	−4.586e−4	0	0
	α	7.5788e−6	0	6.638e−4	−3.147e−6	0
Stainless steel	E	201.04e+9	0	3.079e−4	−6.534e−7	0
	α	12.330e−6	0	8.086e−4	0	0

Table 2
Comparisons of buckling temperatures T_{cr} (in K) for perfect FGM cylindrical shells of Type A with temperature-independent or temperature-dependent properties ($R/t = 400$, $\overline{Z} = 300$ and $T_0 = 300$ K)

Volume fraction index N	Si_3N_4/SUS304		ZrO_2/Ti–6Al–4V	
	T-ID (3,17)[a]	T-D (3,17)	T-ID (3,17)	T-D (3,17)
0.0	386.6576	382.2661	491.2673	491.2673
0.2	396.0286	390.6354	448.6134	442.2616
0.5	406.5425	399.8903	419.5122	402.9180
1.0	418.4561	410.2505	399.5912	383.4589
2.0	432.4454	422.2118	385.6456	371.3242
3.0	440.6835	429.1533	380.3707	366.8971
5.0	450.2794	437.1468	376.1374	363.3554

[a] The number in brackets indicate the buckling mode (m, n).

Table 3
Comparisons of buckling temperatures T_{cr} (in K) for perfect FGM cylindrical shells of Type B with temperature-independent or temperature-dependent properties ($R/t = 400$, $\overline{Z} = 300$ and $T_0 = 300$ K)

Volume fraction index N	$SUS304/Si_3N_4$		$Ti–6Al–4V/ZrO_2$	
	T-ID (3,17)[a]	T-D (3,17)	T-ID (3,17)	T-D (3,17)
0.0	477.6268	459.4390	371.4163	359.1458
0.2	450.8366	437.6332	378.5620	365.0509
0.5	432.2022	422.0153	387.4075	372.6016
1.0	418.4561	410.2505	399.5912	383.4589
2.0	407.9799	401.1375	417.9189	401.2534
3.0	399.0110	397.1830	430.7708	415.4941
5.0	395.7186	393.2538	447.0620	437.9041

[a] The number in brackets indicate the buckling mode (m, n).

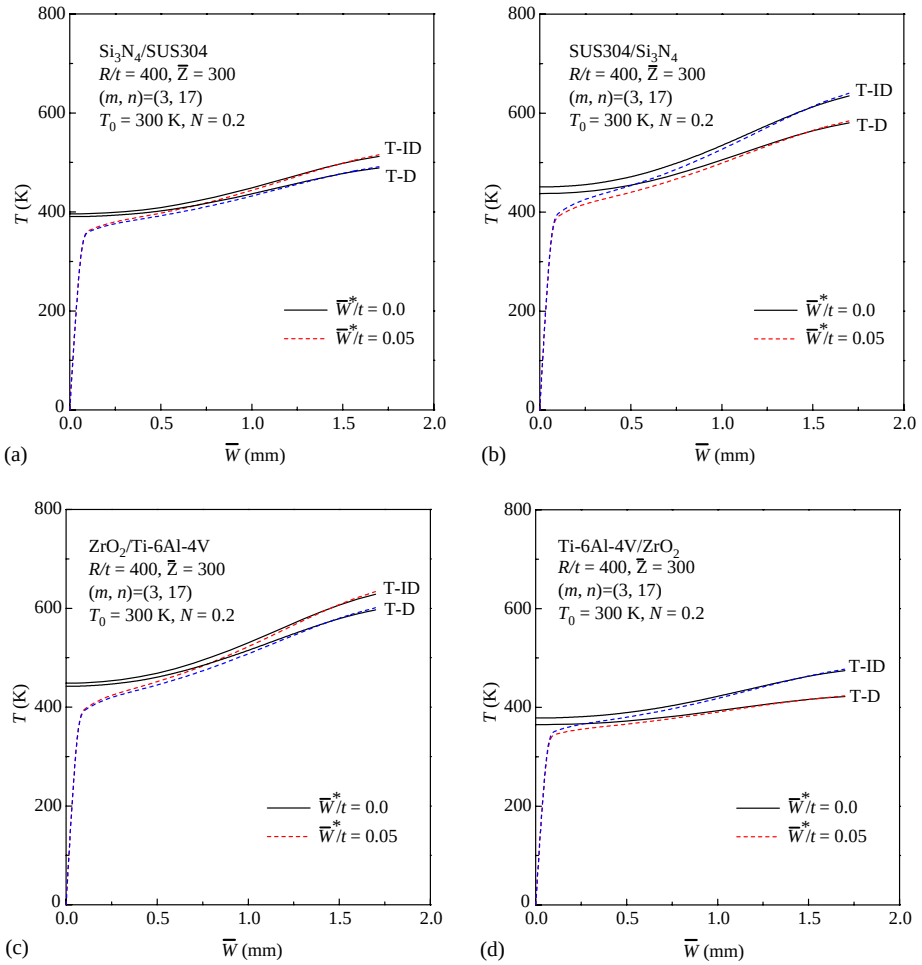

Fig. 1. Effect of material properties on the thermal postbuckling behavior of FGM cylindrical shells. (a) $Si_3N_4/SUS304$ shells, (b) $SUS304/Si_3N_4$ shells, (c) $ZrO_2/Ti–6Al–4V$ shells, (d) $Ti–6Al–4V/ZrO_2$ shells.

(3) Use the temperature determined in the previous step, the temperature-dependent material properties may be decided from Eq. (34) and the thermal buckling load is obtained again.
(4) Repeat step 3 until the thermal buckling temperature converges.
(5) Specify the new value of $\overline{W}/t$, and steps (2)–(4) are repeated until the thermal postbuckling temperature converges.

The thermal buckling loads T_{cr} (in K) for simply supported, perfect FGM cylindrical shells of Types A and B with different values of volume fraction index N subjected to a uniform temperature rise are calculated and compared in Tables 2 and 3. In computation, the shell radius-to-thickness ratio is $R/t = 400$, $\overline{Z} = 300$ and $t = 1$ mm. Note that N in Table 2 represents the volume fraction index of metal while in Table 3 it represents the volume fraction index of ceramic. It can be seen that, for the Si_3N_4/SUS304 and SUS304/Si_3N_4 cylindrical shells, a fully metallic shell ($N = 0$ in Table 2) has the lowest buckling temperature and a fully ceramic shell ($N = 0$ in Table 3) has the largest buckling temperature. Also, the buckling temperature

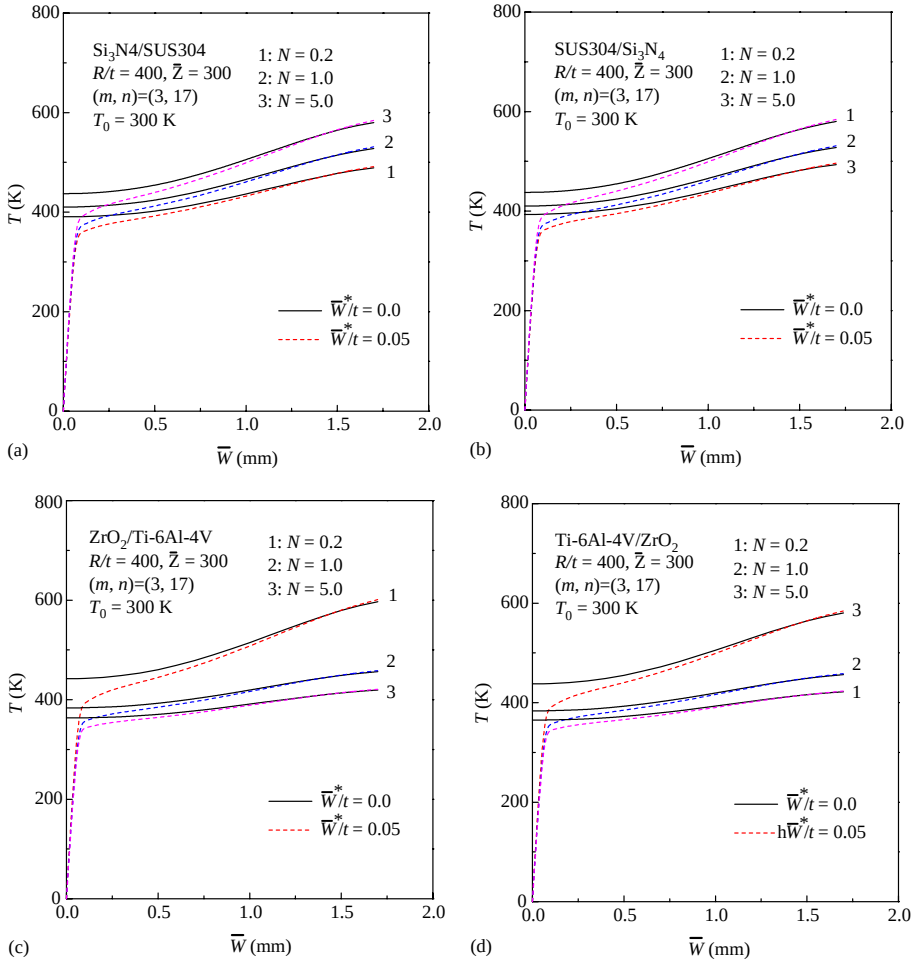

Fig. 2. Effect of volume fraction index N on the thermal postbuckling behavior of FGM cylindrical shells. (a) Si_3N_4/SUS304 shells, (b) SUS304/Si_3N_4 shells, (c) ZrO_2/Ti–6Al–4V shells, (d) Ti–6Al–4V/ZrO_2 shells.

increases as the volume fraction index N of stainless steel increases. This is expected because the metallic shell has a larger value of thermal expansion coefficient α than the ceramic shell does. In contrast, for the ZrO_2/Ti–6Al–4V and Ti–6Al–4V/ZrO_2 cylindrical shells, the buckling temperature is decreased as the volume fraction index N of titanium alloy increases. It can also be seen that the buckling temperature of an FGM cylindrical shell with temperature-dependent material properties (referred to as T-D) is lower than that of the FGM cylindrical shell with temperature-independent material properties (referred to as T-ID). In Tables 2 and 3, (m, n) represent the buckling mode, which determine the number of half-waves in the X-direction and of full waves in the Y-direction.

Fig. 1 shows the thermal postbuckling load–deflection curves for perfect and imperfect, FGM cylindrical shells of Types A and B with a volume fraction index $N = 0.2$ under two cases of thermoelastic material properties, i.e. T-ID and T-D. It can be seen that the thermal postbuckling equilibrium path becomes lower when the temperature-dependent properties are taken into account.

Fig. 2 shows the thermal postbuckling load–deflection curves for the same four FGM cylindrical shells with different values of the volume fraction index N ($= 0.2$, 1.0 and 5.0) when subjected to a uniform temperature rise under T-D case. It can be seen that the Si_3N_4/SUS304 shell has lower buckling temperature and postbuckling path when it has lower volume fraction index N of stainless steel. In contrast, for the ZrO_2/Ti–6Al–4V cylindrical shell, both buckling temperature and thermal postbuckling loads decrease as the volume fraction index N of titanium alloy increases. Note that FGM cylindrical shells of Types A and B, e.g. Si_3N_4/SUS304 and SUS304/Si_3N_4, will have the same thermal postbuckling load–deflection curves when the volume fraction index $N = 1.0$.

It is noted that in all these figures $\overline{W}^*/t$ denotes the dimensionless maximum initial geometric imperfection of the shell. From Figs. 1 and 2, it can be seen that the thermal postbuckling equilibrium path is stable and the shell structure is virtually imperfection-insensitive for both T-ID and T-D cases.

5. Concluding remarks

In order to assess the effects of temperature-dependent material properties and volume fraction index on the thermal postbuckling behavior of FGM cylindrical shells, a fully nonlinear postbuckling analysis is presented based on classical shell theory with a von Kármán–Donnell-type of kinematic nonlinearity. Material properties are assumed to be nonlinear functions of temperature, and graded in the thickness direction according to a simple power law distribution in terms of the volume fractions of the constituents. The boundary layer theory of shell buckling has been extended to the case of FGM cylindrical shells subjected to a uniform temperature rise. A singular perturbation technique is employed to determine buckling temperature and postbuckling load–deflection curves. Numerical results are for two types of FGM cylindrical shell with two constituent materials. In effect, the results provide information about thermal postbuckling behavior of FGM shells for different proportions of the ceramic and metal. The results reveal that the shell has lower buckling temperature and postbuckling load–deflection curves when the temperature-dependent properties are taken into account. They also confirm that the thermal postbuckling equilibrium path is stable and the shell structure is virtually imperfection-insensitive.

Acknowledgement

This work is supported in part by the National Natural Science Foundation of China under Grant 50375091. The author is grateful for this financial support.

Appendix A

In Eq. (18)

$$A_x^T = \frac{t}{1-v}\left\{(\alpha_i-\alpha_o)(E_i-E_o)\frac{1}{2N+1} + [\alpha_o(E_i-E_o)+(\alpha_i-\alpha_o)E_o]\frac{1}{N+1} + \alpha_o E_o\right\} \tag{A.1}$$

and in Eqs. (32) and (33)

$$\begin{aligned}
\Theta_3 &= \frac{1}{C_3}\left\{\left(\frac{\gamma_{24}^2}{\gamma_{14}\gamma_{24}+\gamma_{34}^2}\right)\frac{m^4(1+\propto)}{16n^2\beta^2 g_2}\varepsilon^{-1}\right.\\
&\quad \left.+\frac{1}{32}\left(\frac{\gamma_{24}^2}{\gamma_{14}\gamma_{24}+\gamma_{34}^2}\right)\frac{m^2}{\gamma_{24}n^2\beta^2}\left[\frac{\gamma_{34}}{\gamma_{24}}(1+2\propto)-2\gamma_{24}\frac{g_3}{g_2}\right]+\frac{\gamma_{24}^2-\gamma_5^2}{\gamma_{24}}\frac{\gamma_{T2}}{g_T}\lambda_T^{(2)}\right\}\\
\Theta_4 &= \frac{\gamma_{24}^2-\gamma_5^2}{\gamma_{24}}\frac{\gamma_{T2}}{g_T}\lambda_T^{(0)}\\
\lambda_T^{(0)} &= \left\{\frac{\gamma_{24}m^2}{(1+\propto)g_2}\varepsilon^{-1}+\gamma_{24}\frac{(2+\propto)g_3}{(1+\propto)^2 g_2}\right.\\
&\quad \left.+\frac{1}{(1+\propto)m^2}\left[\frac{g_1}{\gamma_{14}}+\frac{\gamma_{24}}{(1+\propto)^2}\frac{g_3^2}{g_2}\right]\left[1-\frac{\propto}{1+\propto}\frac{g_3}{m^2}\varepsilon\left(1-\frac{\propto}{1+\propto}\frac{g_3}{m^2}\varepsilon\right)\right]\varepsilon\right\}\\
\lambda_T^{(2)} &= \left\{\left(\frac{\gamma_{24}^2}{\gamma_{14}\gamma_{24}+\gamma_{34}^2}\right)\frac{\gamma_{24}m^6}{4g_2^2}\varepsilon^{-1}\right.\\
&\quad +\left(\frac{\gamma_{24}^2}{\gamma_{14}\gamma_{24}+\gamma_{34}^2}\right)\frac{m^4}{8g_2}\left[\frac{\gamma_{34}}{\gamma_{24}}\frac{(1+\propto)^2+(1+2\propto)}{1+\propto}\right]\\
&\quad -\frac{1}{16}\left(\frac{\gamma_{14}}{\gamma_{14}\gamma_{24}+\gamma_{34}^2}\right)m^2(1+2\propto)\varepsilon+\frac{1}{4}\frac{\gamma_{24}m^2n^4\beta^4}{g_2}\frac{g_2(5+10\propto+2\propto^2)+16m^4(1+\propto)}{g_2(1+\propto)-4m^4}\varepsilon\\
&\quad -\left(\frac{\gamma_{24}^2}{\gamma_{14}\gamma_{24}+\gamma_{34}^2}\right)\frac{m^2}{8g_2}\left[\propto\frac{g_{11}}{\gamma_{14}}+\frac{(2+4\propto+3\propto^2)}{(1+\propto)^2}\frac{\gamma_{34}}{\gamma_{24}}g_3\right]\varepsilon\\
&\quad \left.-\frac{\gamma_{24}}{2g_8}\left[m^2\left(1+2\propto+\frac{1}{\pi\vartheta}\varepsilon^{1/2}\right)\varepsilon-2g_3\varepsilon^2+\frac{g_3^2}{m^2}\varepsilon^3\right]\right\}\\
\lambda_T^{(4)} &= \frac{1}{32}\left(\frac{\gamma_{24}^2}{\gamma_{14}\gamma_{24}+\gamma_{34}^2}\right)^2\frac{\gamma_{24}m^{10}(1+\propto)}{g_2^3}\frac{g_{13}+5g_2(1+\propto)}{g_{13}-g_2(1+\propto)}\varepsilon^{-1}\\
&\quad +\frac{1}{64}\frac{\gamma_{24}}{g_8}\left\{\frac{b}{32\pi\vartheta}\left(\frac{\gamma_{24}^2}{\gamma_{14}\gamma_{24}+\gamma_{34}^2}\right)^2\frac{m^8(1+\propto)^2}{n^4\beta^4 g_2^2}\varepsilon^{-3/2}\right.\\
&\quad \left.+m^2n^4\beta^4(1+\propto)^2\left[\frac{g_2(1+2\propto)+8m^4(1+\propto)}{g_2(1+\propto)-4m^4}\right]^2\varepsilon^3\right\}
\end{aligned} \tag{A.2}$$

in the above equations

$$g_1 = m^4 + 2\gamma_{12}m^2n^2\beta^2 + \gamma_{14}^2n^4\beta^4, \quad g_2 = m^4 + 2\gamma_{22}m^2n^2\beta^2 + \gamma_{24}^2n^4\beta^4,$$
$$g_3 = \gamma_{30}m^4 + \gamma_{32}m^2n^2\beta^2 + \gamma_{34}n^4\beta^4, \quad g_{13} = m^4 + 18\gamma_{22}m^2n^2\beta^2 + 81\gamma_{24}^2n^4\beta^4,$$
$$C_3 = 1 - \frac{g_3}{m^2}\varepsilon, \quad b = \left(\frac{\gamma_{14}\gamma_{24}}{1+\gamma_{14}\gamma_{24}\gamma_{30}^2}\right)^{1/2}, \quad c = -\frac{\gamma_{14}\gamma_{24}\gamma_{30}}{1+\gamma_{14}\gamma_{24}\gamma_{30}^2}, \quad \vartheta = \left[\frac{b-c}{2}\right]^{1/2}, \quad \phi = \left[\frac{b+c}{2}\right]^{1/2}$$
$$C_{11} = \frac{g_8}{g_T}, \quad g_8 = \gamma_{24}^2 - \frac{4}{\pi}\frac{\vartheta}{b}\gamma_5^2\varepsilon^{1/2}, \quad g_T = (\gamma_{24}^2\gamma_{T1} - \gamma_5\gamma_{T2}) + \frac{4}{\pi}\frac{\vartheta}{b}\gamma_5(\gamma_{T2} - \gamma_5\gamma_{T1})\varepsilon^{1/2} \tag{A.3}$$

References

Batdorf, S.B., 1947. A simplified method of elastic-stability analysis for thin cylindrical shells. NACA TR-874.

Birman, V., Bert, C.W., 1993. Buckling and post-buckling of composite plates and shells subjected to elevated temperature. Journal of Applied Mechanics ASME 60, 514–519.

Gibson, L.J., Ashby, M.F., Karam, G.N., Wegst, U., Shercliff, H.R., 1995. Mechanical properties of natural materials. II. Microstructures for mechanical efficiency. Proceedings of the Royal Society of London Series A 450 (1938), 141–162.

Gong, S.W., Lam, K.Y., Reddy, J.N., 1999. The elastic response of functionally graded cylindrical shells to low-velocity impact. International Journal of Impact Engineering 22, 397–417.

Han, X., Liu, G.R., Xi, Z.C., Lam, K.Y., 2001. Transient waves in a functionally graded cylinder. International Journal of Solids and Structures 38, 3021–3037.

Loy, C.T., Lam, K.Y., Reddy, J.N., 1999. Vibration of functionally graded cylindrical shells. International Journal of Mechanical Sciences 41, 309–324.

Ng, T.Y., Lam, K.Y., Liew, K.M., Reddy, J.N., 2001. Dynamic stability analysis of functionally graded cylindrical shells under periodic axial loading. International Journal of Solids and Structures 38, 1295–1309.

Pradhan, S.C., Loy, C.T., Lam, K.Y., Reddy, J.N., 2000. Vibration characteristics of functionally graded cylindrical shells under various boundary conditions. Applied Acoustics 61, 111–129.

Reddy, J.N., Chin, C.D., 1998. Thermoelastical analysis of functionally graded cylinders and plates. Journal of Thermal Stresses 21, 593–626.

Shahsiah, R., Eslami, M.R., 2003. Thermal buckling of functionally graded cylindrical shell. Journal of Thermal Stresses 26, 277–294.

Shen, H.-S., 1997. Thermal postbuckling analysis of imperfect stiffened laminated cylindrical shells. International Journal of Non-Linear Mechanics 32, 259–275.

Shen, H.-S., 2002a. Thermal postbuckling analysis of laminated cylindrical shells with piezoelectric actuators. Composite Structures 55, 13–22.

Shen, H.-S., 2002b. Postbuckling analysis of axially-loaded functionally graded cylindrical shells in thermal environments. Composites Science and Technology 62, 977–987.

Shen, H.-S., 2003. Postbuckling analysis of pressure-loaded functionally graded cylindrical shells in thermal environments. Engineering Structures 25, 487–497.

Shen, H.-S., Chen, T.-Y., 1988. A boundary layer theory for the buckling of thin cylindrical shells under external pressure. Applied Mathematics and Mechanics 9, 557–571.

Shen, H.-S., Chen, T.-Y., 1990. A boundary layer theory for the buckling of thin cylindrical shells under axial compression. In: Chien, W.Z., Fu, Z.Z. (Eds.), Advances in Applied Mathematics and Mechanics in China, vol. 2. International Academic Publishers, Beijing, China, pp. 155–172.

Touloukian, Y.S., 1967. Thermophysical Properties of High Temperature Solid Materials. McMillan, New York.